Optimized Lung Cancer Detection and Classification Using Attention Based CNN Driven Improved Chan-Vese Algorithm

A.J. Rajeswari Joe*[1], V. Thamilarasi[2], Akhilesh Singh[3], Udhayakumar S[4], R. Rajiniganth[5], Ezhil Arasu[6]

[1]Department of Computer Science (PG & Research), Thiruthangal Nadar College, Chennai, India.
[2]Assistant Professor of Computer Science, Sri Sarada College for Women (Autonomous), Salem-16, Tamilnadu, India.
[3]Department of Electrical Engineering, Uttarakhand Technical University Campus Institute (NPSEI) Pithoragarh, Uttarakhand, India.
[4]Assistant Professor, Department of Electronics and Communication Engineering, KGiSL Institute of Technology, Coimbatore, India.
[5]Assistant Professor, Department of Computer Science and Technology, SNS College of Technology, Coimbatore, India.
[6]Associate Professor, SNS College of Physiotherapy, SNS Kalvi Nagar, Sathy Main Road, Kurumbapalayam, Coimbatore, India.
rajeswarijoe.aj@thiruthangalnadarcollege.edu.in

Abstract. Globally, lung illness is the leading cause of death. Lung cancer is the leading cause of mortality for both people and has the most startling death rate of all tumour kinds. An estimated 1.1 million individuals die from this disease each year, while an estimated 1.2 million people receive a routine diagnosis. Early cancer detection increases the survival rate. It is difficult to immediately identify malignant growths in the lungs. Lung cancer can be detected using a variety of imaging techniques. A radiologist can predict and detect abnormalities with speed and accuracy by using a computer-aided diagnosis technique. The main goal of the CAD systems is to locate lung nodules. Since the course of treatment depends on the stage of the disease, it is imperative to focus on staging lung cancer as soon as it is discovered. The accuracy of lung cancer staging and nodule segmentation is one of the primary issues with existing CAD systems. The primary objective of the proposed work is to segment the lung nodule from the CT image and classify it as malignant or non-cancerous in order to diagnose the site of cancer with more sensitivity, specificity, and accuracy than current methods.

Keywords: Boosted Adaptive Diffusion filter, fuzzy Thresholding, optimized chan-vese algorithm, 3D-CNN.

S. P. Vijayaragavan et al. (eds.), *Proceedings of the Global Conference on Sustainable Energy Systems, Smart Electronics and Intelligent Computing (GCSESEIC 2025)*, Advances in Engineering Research 297,
https://doi.org/10.2991/978-94-6239-654-8_63

1. Introduction

Lung cancer is the second most common cause of mortality globally. Early identification of lung cancer is essential for patient care and enhances the chance of survival [2]. To identify lung cancer early, researchers develop complex algorithms. A new strategy is being proposed to protect individuals against the deadly disease [3]. Early detection of lung cancer improves treatment and survival. Due to genetics and lifestyle decisions, it affects millions of individuals globally. The WHO reported 2.2 million new cases and 1.8 million fatalities in 2020 [1]. Treatment and early detection can lower these rates and improve survival. Nicotine from cigarettes is the cause of lung cancer. Lung cancer is spread via asbestos exposure, air pollution, and passive smoking [4]. Lung cancer has an impact on family and daily life. Coughing, dyspnea, and chest pain cause emotional, physical, and financial difficulties for patients with lung illness. Lung cancer causes death, lost productivity, and medical expenses. Patients with lung cancer require critical care.

2. Research Gap Identified

Early detection is essential for lowering cancer mortality [5]. Early detection of cancer stops it from spreading widely. Early intervention improves survival and is more successful. Early cancer detection increases quality of life, minimizes intrusive therapies, and protects organ function.

The primary goal of the project is to create an Auto-Detective Computed Aided Diagnostic (AD-CAD) model that uses the following technique to identify lung nodules in CT scans:

- To use cutting-edge optimization and classification methods to detect and categorize lung cancer lesions.
- When creating the algorithm, parameters like variance and mean standard error are taken from the region of interest and compared to the current method.
- The segmented image's features are extracted using a feature extraction technique;
- A unique classification is proposed to increase accuracy and lessen the time consumption problem.
- To reduce the proportion distribution of lung cancer and avoid severe stages in early.

The following is a description of the work: In section 1, the introduction is presented together with the studies of many research publications; in part 2, the recommended approach is highlighted; and in part 3, performance indicators are defined. The research findings are presented in Part 4, and the task is finished in Part 5.

3. Proposed Work

By creating a hybrid strategy using the watershed algorithm and random walk, this study seeks to increase segmentation accuracy. In the random walk algorithm pixels are selected as initial seed points for the object and background and are labeled. The remaining unlabeled pixels are either marked as object or background. This may be done by calculating the probability of unlabeled reaching the seed points. Then a vector of probabilities is calculated for each unlabeled pixel. Based on the probability obtained it may label either as object or background. It is a challenging task to select an effective feature set and a proper machine learning based classifier for medical images. An essential first step in the detection and classification of lung cancer is texture analysis of CT scans [6]. A CAD uses this extracted feature values from the texture to differentiate the cancer type as malignant or benign.

3.1 Image Acquisition

A growing body of research suggests that computer vision approaches may be able to beat radiologists in terms of speed and accuracy, even though radiologists have been performing the aforementioned medical imaging duties [7]. “In this case, the DICOM picture format is being converted to JPEG format using converters. For a better function, the image size is usually converted from 512 x 512 to 256 x 256. This suggested method uses 150 pictures, both tumor and non-tumor, for diagnosis.

3.2 IMAGE PREPROCESSING:

Boosted Anisotropic Diffusion Filter: The first step involves preprocessing the images Fig 1. Preprocessing includes eliminating the nose from the image, separating the lung region from the CT slice, and applying filters to improve the image's quality [8]. The following PDE guiding mechanism serves as the foundation for the traditional linear smoothing method known as anisotropic filtering equation (1).

$$\frac{\partial I_m}{\partial t} = div(T\nabla I_m) \tag{1}$$

In the weighting direction m, where I_m is the image strength, ∇ is a gradient operator, t is the time, and div is a divergence operator. The directionality of smoothing is provided by the tensor of structure T Equation (2). It is built using a common gradient tensor G that is produced by convolving the total of the outer products of ∇I_m using a Gaussian kernel across all weighting directions K_ρ:

$$G = k_p * \sum_m (\nabla I_m \oplus \nabla I_m) \tag{2}$$

where $\otimes$ symbolizes the operator for the outside product [9]. The Gaussian kernel's standard deviation, or parameter ρ, determines the gradient tensor's spatial scale equation (3).

$$f_k^*(x_k) = \sum_{i=1}^{L_k^*} \omega_{k,i}^* \,.\, N\left(x_k; x_{k,i}^*, C_{k,i}^*\right), with\ * \in [e,p] \tag{3}$$

for every time step k, where L_k^* is the number of mixture components.

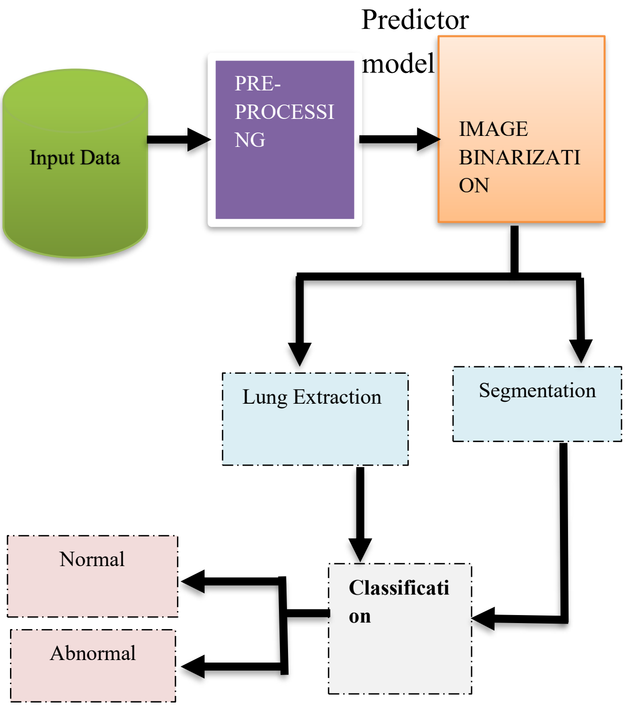

Fig 1: Overall, View of Proposed Work

3.3 IMAGE BINARIZATION

The model is trained using the preprocessed data and the selected features in order to identify trends and relationships between the input features and the pertinent lung cancer categories. Following training, the classification model's performance and capacity for generalization are assessed [10]. This is usually accomplished by using cross-validation techniques or by dividing the dataset into training and testing sections. Evaluation measures gauge the model's effectiveness.

Rather, before rendering a final decision, each radiologist examined both their own scores and the anonymous scores of three other radiologists. This method finds every lung nodule on a CT scan as completely as possible and takes into account the opinions of several specialists without enforcing a mandatory agreement.

3.4 Lung Extraction

Too far, numerous methods for fissure identification and lobe segmentation have been developed. finds the most likely fissure locations in 2D slices using a graph search after determining likely (oblique) fissure locations using fuzzy sets [11]. The results were reported on normal subjects, and the approach necessitates manual initialization. To create a distance map, they must first get a vessel segmentation. Watershed segmentation of the lobes is driven by the distance map, the original image, and user input. Segment the lobes in a similar manner, but seed the watershed segmentation in an automated framework using a segmented airway tree. Create ridge maps to highlight features, then de-lineate them using active open contours. In their investigation, ten patients with pulmonary nodules were examined. About 2.4% of the secure zones required manual adjustment, and algorithm run times were roughly five minutes. To segment the lobes, they employ deformable mesh models [12]. The convex hull model is not as effective as the concave hull model. Digging is necessary to create a concave hull with the proper profundity, and the concave hull is calculated using the known value of the convex hull technique.

The suspected areas are enhanced while other structures, such as blood vessels, are suppressed in order to identify the potential nodules during the nodule found stage. This stage narrows the nodule detection search space [13]. Nodule segmentation is a very crucial and important step in the CAD system. This process delineates the focused nodule regions in the CT images. Various features can be extracted for further analysis from a local image area defined by this segmentation. Fig 1 depicts the nodule segmentation process outcomes. The next step is to determine if the nodules are benign or cancerous after they have been segmented. The features taken from the nodules are used for this [14]. Features include the nodule's size, shape, and appearance as well as its growing pace. Nodules smaller than one centimeter are probably benign, but those larger than one centimeter are probably cancerous. Benign nodules are round in appearance, while malignant nodules are lobulated, speculated, ragged, and halo-shaped. Malignant nodules typically have an irregular surface, whereas benign nodules typically have a uniform surface. Malignant nodules grow more quickly than benign modules in terms of growth rate. One of the fatal illnesses that needs to be predicted in order to lower the fatality rate is lung cancer. In order to improve accuracy automatically, artificial intelligence is used to CT scan images. One of the newest approaches to value prediction is deep learning. Convolution Neural Networks, one of the deep learning techniques used to sample, produce better outcomes than other machine learning algorithms. Batch normalization for a transformed feature-map F_l^k is shown in equation (4).

$$N_l^k = \frac{F_l^k - \mu_B}{\sqrt{\sigma_B^2 + \varepsilon}} \quad (4)$$

The objective is to validate our lung cancer prediction since early detection is essential for effective therapy [15]. CNN was first trained using screening data from the US using an independent multicenter dataset from Europe. In order to improve early detection with dependable machine learning models and save lives, this study investigates early-stage lung cancer diagnosis using CNNs. Each variable's contribution can be written to the cFhain rule Equation (5).

$$\frac{\partial e}{\partial x_{i,j,k}^{\ell}} = \frac{\partial e}{\partial y_{i,j,k}^{\ell}} \frac{\partial f(y_{i,j,k}^{l})}{\partial y_{i,j,k}^{\ell}} = \frac{\partial e}{\partial y_{i,j,k}^{\ell}} f'(x_{i,j,k}^{l}) \quad (5)$$

Although CNN models have shown excellent accuracy on controlled datasets, there is still a significant obstacle to their application in real-world situations involving a variety of patient groups. To address this, robustness against unanticipated differences in imaging data must be ensured through validation across numerous datasets and techniques Equation (6).

$$\frac{\partial e}{\partial y_{i,j,k}^{\ell-1}} = \sum_{a=0}^{n1-1} \sum_{b=0}^{n2-1} \sum_{c=0}^{n3-1} \frac{\partial e}{\partial x'_{(i-a),(j-b),Uk-c)}} \frac{\partial x_{(i-a)(j-b)(j-b)}^{\ell}}{\partial y_{i,j,k}^{\ell-1}}$$
$$= \sum_{a=0}^{n1-1} \sum_{a=0}^{nz-1} \sum_{b=0}^{n3-1} \frac{\partial e}{\partial x_{(i-a)(j-b),(k-c)}^{T}} \omega_{a,b,c^*} \quad (6)$$

This technique automatically extracts self-learned features using end-to-end learning CNN, outperforming conventional methods and conventional computer-aided diagnosis systems.

3.5 Classification: Convolutional Neural Network

The deep learning neural network model is a neural network with numerous layers of nodes between the input and output layers that employs the deep learning technique [16]. Similar to this, in order to recognize and process the corresponding inputs, the deep learning architecture is built using several series of interconnected layers between the inputs and outputs [17]. All networks with a single hidden layer, including the deep multi-layer perceptron model, deep recurrent neural network model, deep convolutional neural network model, deep adaptive neural network model, and others, are subject to the deep learning (DL) technique.

The 3D input CNN x assumes to calculate the non-linear input $x_{i,j,k}^{\ell}$ to (i, k) th unit in the level ℓ, the following is added Equation (7).

$$x_{i,j,k}^{\ell} = \sum_a \sum_b \sum_c \omega_{a,b,c} y_{(i+a)(j+b)(k+c)}^{\ell-1} + b^{\ell} \quad (7)$$

The result of the $(i,j)^{th}$unit in the ℓ^{th} This is how the convolutional layer appears:

$$y_{i,j,k}^{\ell} = f(x_{i,j,k}^{\ell}) \quad (8)$$

Lung cancer is also significantly influenced by hereditary factors Equation (8). Lung cancer is caused by unchecked tissue multiplication [16]. Both malignant and noncancerous lung cancers are possible Equation (9).

$$f_1^k(p,q,r) = \sum_c \sum_{x,y,z} i_c(x,y,z) \,.\, e_1^k(u,v,w) \quad (9)$$

The expression for a convolutional operation is

$$F_1^k = [f_1^k(1,1,1), \ldots (f_1^k(p,q,r), \ldots f_1^k(P,Q,R))] \quad (10)$$

This study developed an automated technique for exploiting grayscale CT scan pictures to diagnose malignancy Equation (10,11).

$$Z_l^k = g_p\left(F_l^k\right) \quad (11)$$

The activation function for a convolved feature-map is defined by equation (11).

$$T_l^k = g_a(F_l^k) \quad (12)$$

The equation above F_l^k is a output of convolution that is allocated to the activation function g_a (.) that transforms the output and adds non-linearity T_l^k for lth layer Equation (12).

4. Experimental Results & Discussion

This innovative technique for automatic lung cancer identification from CT scans makes use of a 2D CNN with Taguchi optimization Fig 2,3. It significantly improves classification accuracy by carefully adjusting CNN settings using 36 tests and 8 control factors Fig 4,5. Additionally, by combining convolutional and bidirectional recurrent neural networks into a special deep learning model, accuracy was increased utilizing the NSCLC Radio genomics dataset with people as mentioned in reference.

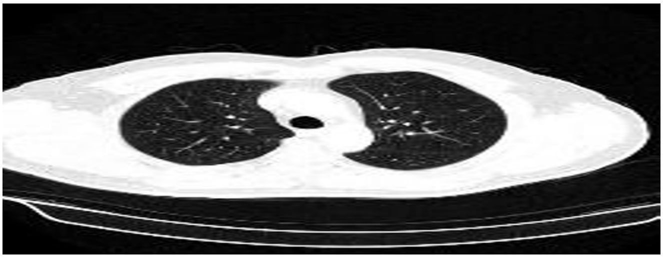

Fig 2: Lung monitoring

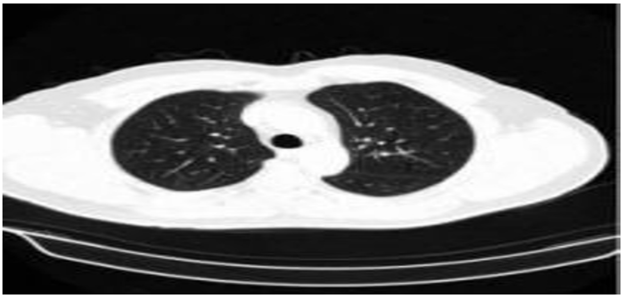

Fig 3: Input Image

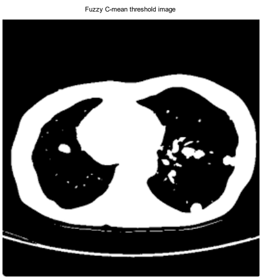

Fig 4: Lung efficiency

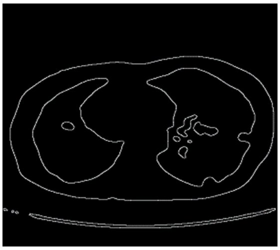

Fig 5: Muscle activity monitoring

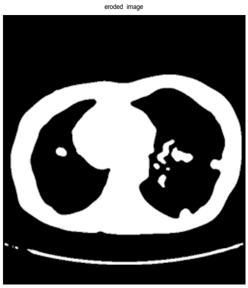

Fig 6: HRV estimation lung

Fig 7: Physiological states

Fig 8: lung breathing

Fig 9: Lung extraction result

Since it has been demonstrated that these models have produced highly successful results, Fig 6,7 illustrates the goal of this work, which is to develop a CNN to identify different categories of lung patterns in Fig 8,9.

Fig 10: Breathing analysis

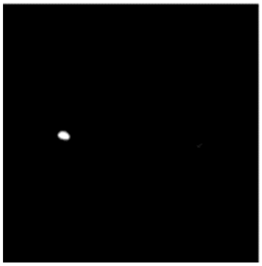

Fig 11:preventive care

Fig12: Lung function

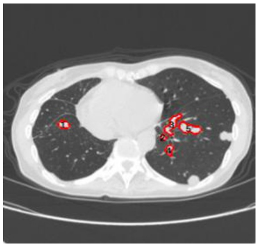

Fig 13: Result of Segmentation

After the extraction procedure, certain innovative techniques are used to segment the data Fig 10,11. When compared to conventional segmentation techniques this innovative method performs better Fig 12,13.

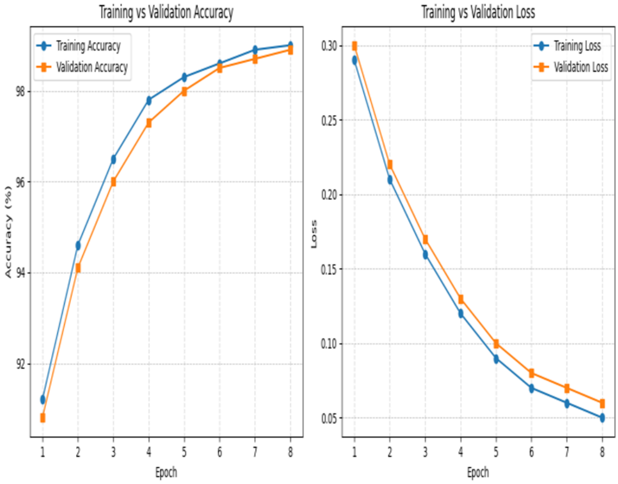

Fig 14: Training Vs accuracy and Loss

These two methods perform well, but they have a few drawbacks: they over segmented the image and missed small nodules Fig 14. The optimization model is used to solve these issues. This recommended improved method effectively labels the nodule, accurately separates the image with hazy boundaries, and clearly distinguishes the shapes.

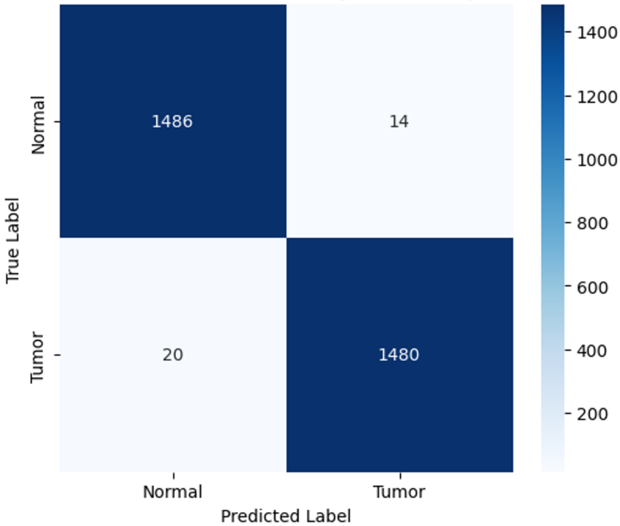

Fig 15: Confusion matrix of 3D-CNN

The development of CNN-based models that outperform human recognition capabilities and produce high-accuracy results has significantly advanced image categorization and its applications Fig 15.

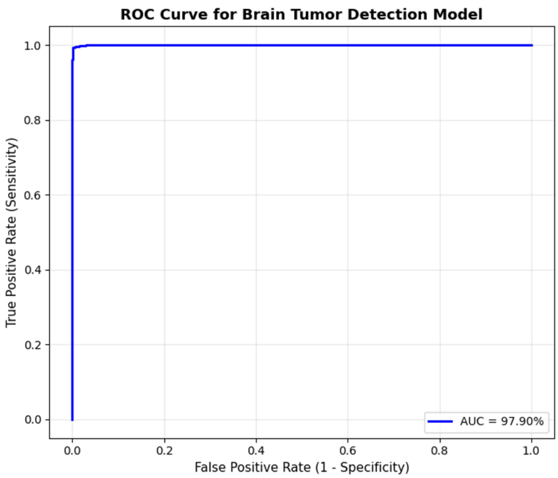

Fig 16: Roc curve and PR curve

However, one of the most promising uses of DL for cancer detection and tumor exploration is the use of such models in medical picture analysis Fig 16.

A set of images that represent a historical chronology must be closely analyzed in order to generate new frames and anticipate the appearance of anomalies. It is also essential to concentrate on picture recognition and analysis in order to enhance productivity and avoid needless effort.

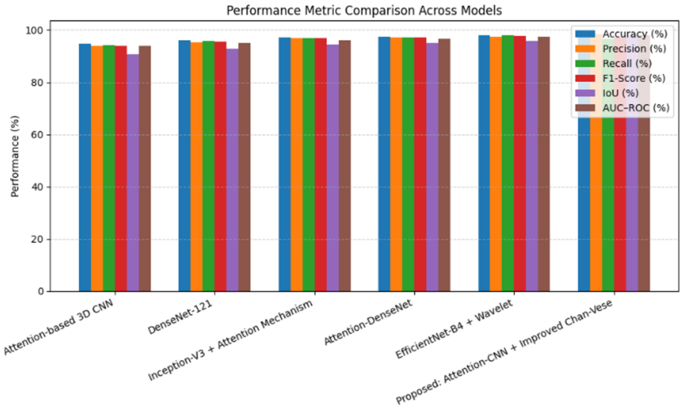

Fig 17: Performance Comparison

The goal is to create unique models that can identify the body part and tomographic plane seen in each frame Fig 17. By examining the composition of these images, important information about the connections between their different parts can be found, improving knowledge of intricate anatomical systems for more precise diagnosis and treatment recommendations.

5. Conclusion

The suggested system uses a variety of image processing methods and classification algorithms to automatically identify lung tumors. After a number of preprocessing techniques are applied to the lung pictures, the outcomes are shown. After that, segmentation is finished. Lastly, the suggested classifiers are used to categorize lung tumor phases, such as benign and malignant. The recommended approach produces considerably superior results. The suggested system classifies the different stages of lung cancer. The procedure typically requires three steps to complete. Lung cancer patients must be screened in order to prevent death. The lung abnormalities are identified using sophisticated detection algorithms and medical image processing procedures.

References

1. Bray, Freddie, Jacques Ferlay, Isabelle Soerjomataram, Lindsey A. Torre, Rebecca L. Siegel, Ahmedin Jemal. "World cancer statistics 2018: GLOBOCAN reports the prevalence and mortality of 36 cancers globally in 185 countries." CA: Clinician Cancer Journal 68, No. 6: 394-424. (2018)

2. Ramaswamy Govindan, Morgensztern, Daniel, Shean Huey Ng, Feng Gao. "Trends in the stage distribution of non-small cell lung cancer patients: a National Cancer Database Survey." Thoracic Oncology Journal 5, No. 1: 29-33. (2010)
3. Weinberg, Robert A. Cancer Biology: Second Student Edition International. WW Company & Norton, 2013.
4. Bhuvaneswari, C., P. Aruna, and D. Loganathan. "A new fusion model for classification of the lung diseases using genetic algorithm." Egyptian Informatics Journal 15, no. 2: 69-77. (2014)
5. Ajin, M., and L. Mredhula. "Diagnosis of Interstitial Lung Disease by Pattern Classification." Procedia computer science 115: 195-208. (2017)
6. Roy, Tanushree Sinha, Neeraj Sirohi, and Arti Patle. "Classification of lung image and nodule detection using fuzzy inference system." In International Conference on Computing, Communication & Automation, pp. 1204-1207. IEEE, 2015.
7. Ignatious, Sruthi, and Robin Joseph. "Computer aided lung cancer detection system." In 2015 Global Conference on Communication Technologies (GCCT), pp. 555-558. IEEE, 2015.
8. Rendon-Gonzalez, Elmar, and Volodymyr Ponomaryov. "Automatic Lung nodule segmentation and classification in CT images based on SVM." In 2016 9th International Kharkiv Symposium on Physics and Engineering of Microwaves, Millimeter and Submillimeter Waves (MSMW), pp. 1-4. IEEE, 2016.
9. Bhuvaneswari, P., and A. Brintha Therese. "Detection of cancer in lung with k-nn classification using genetic algorithm." Procedia Materials Science 10: 433-440. (2015)
10. Lakshmanaprabu, S. K., Sachi Nandan Mohanty, K. Shankar, N. Arunkumar, and Gustavo Ramirez. "Optimal deep learning model for classification of lung cancer on CT images." Future Generation Computer Systems 92: 374-382. (2019)
11. Alves, Jeovane H., Pedro M. Moreira Neto, and Lucas F. Oliveira. "Extracting Lungs from CT Images using Fully Convolutional Networks." In 2018 International Joint Conference on Neural Networks (IJCNN), pp. 1-8. IEEE, 2018.
12. Sinthia, P., M, Malathi., T, Sripriya., Krishnan, R., G, Gurumoorthy., Jalaldeen, K.: Monitoring vital parameters of comatose patients using smart sensors integrated with cloud storage. (2024). https://doi.org/10.1109/i-smac61858.2024.10714845.
13. Nithila, Ezhil E., and S. S. Kumar. "Segmentation of lung from CT using various active contour models." *Biomedical Signal Processing and Control* 47: 57-62. (2019)

14. Lee, Howard, and Yi-Ping Phoebe Chen. "Image based computer aided diagnosis system for cancer detection." *Expert Systems with Applications* 42, no. 12: 5356-5365. (2015)
15. Taher, Fatma, and Rachid Sammouda. "Lung cancer detection by using artificial neural network and fuzzy clustering methods." In *2011 IEEE GCC Conference and Exhibition (GCC)*, pp. 295-298. IEEE, 2011.
16. Rendon-Gonzalez, Elmar, and Volodymyr Ponomaryov. "Automatic Lung nodule segmentation and classification in CT images based on SVM." In 2016 9th International Kharkiv Symposium on Physics and Engineering of Microwaves, Millimeter and Submillimeter Waves (MSMW), pp. 1-4. IEEE, 2016.
17. V. Thamilarasi, A. Asaithambi, R. Roselin, " Enhance ensemble segmentation of ling chest X-Ray images by denoising autoencoder and CLAHE", ICTACT Journal on Image and Video Processing, Volume: 15 , Issue: 3 , Pages: 3501 - 3508, , 10.21917/ijivp.2025.0496. 2025